Ion nitriding of explosively-clad titanium/steel tandems

H. AKBULUT
Sakarya University, Engineering Faculty, Department of Metallurgy and Materials Engineering, Esentepe Campus, Sakarya 54040, Turkey

O. T. INAL, C. A. ZIMMERLY
Materials and Metallurgical Engineering, New Mexico Tech, Socorro, New Mexico 87801, USA

Ti-6Al-4V, that was explosively welded to a 304 stainless steel plate, was ion nitrided in a d.c. plasma. An effective nitriding was achieved due to the high dislocation density and vacancy concentration that emaneted from the shock wave exposure of explosive welding which, in turn, accelerated diffusion of nitrogen into the titanium matrix. Processed Ti-6Al-4V developed a surface layer of TiN (δ) followed by a Ti_2N (ε) and interstitial nitrogen containing diffusion layer of α-titanium. The growth rate of compound layer ($\delta + \varepsilon$) and case depth were found to be controlled by the diffusion of nitrogen. Depending on the temperature of ion nitriding, high Knoop hardness values, between 800 and 2520, were obtained and these values show two to sixfold increase in the hardness when compared with unprocessed samples. XRD results showed VN formation also, together with TiN and Ti_2N nitrides and a preferred TiN growth in (002) orientation. Interfaces between Ti-6Al-4V and 304 stainless steel showed higher hardnesses as was seen following explosive welding than associated cores and a small amount of recrystallization was observed in the Ti-6Al-4V layer at the higher temperature processing. Nitriding of clad-Ti-6Al-4V thus provides an excellent opportunity of cladding surfaces with titanium alloys, in advanced structural applications without the expense of their monolithic counterparts. © *1999 Kluwer Academic Publishers*

1. Introduction

The remarkable strength-to-weight ratios of titanium alloys has resulted in their acceptance in aircraft and aerospace applications which, in turn, has reduced their prices to levels where their superior corrosion and erosion resistance, as well as antifouling properties, enabled their use in chemical process industries [1].

Explosive welding is one example of a constructive application of explosives in which the energy produced by the detonating explosive is used to accelerate a metal plate (flyer plate) across a predetermined distance (stand-off-distance) into contact with another metal plate (base plate) and achieve a solid-state joining. Explosive welding affords the welding of two or more similar or dissimilar metals. Metal plates can range from a few square inches in area to a couple of hundred square feet. At the collision point, pressures in the millions of psi are generated as well as strain rates of $10^6 \, s^{-1}$. Due to the high pressures and associated strain rates, a phenomenon known as jetting occurs. Jetting allows for the removal of the oxide layer present at the weld surfaces of the plates, leaving behind perfectly clean surfaces. Under the high pressures generated by the colliding plates, the clean surfaces are forced into intimate contact and a metallurgical bond is formed [2, 3].

Ion nitriding, utilizing a N_2-Ar glow discharge plasma, is one of the effective methods for the surface hardening of Ti alloys [4]. With this treatment, a diffusion layer, with a high hardness, is formed on the specimen surface and resistance to wear and fatigue is improved. Ion nitriding affords many advantages, such as the elimination of environmental pollution and energy savings over conventional salt bath nitriding and gas nitriding [5, 6].

Titanium nitride is of great technological interest owing to its unique characteristics such as extreme hardness, high chemical and physical stability, good thermal and electrical conductivity and high melting point [7]. Titanium nitride can also be a good contact material for semiconductors and a promising candidate material for fusion reactors [8]. Moreover, nitriding makes titanium very versatile. Ti and its alloys posses excellent strength-to-weight ratios, fracture toughness, corrosion resistance and bicompatibility. Nitriding of titanium and its alloys can improve their wear characteristics [9] and fatigue crack initiation resistance [10] and has a great potential to expand the field of applications for this class of materials. Such applications include tribological and orthopedic devices, gears, valves, pumps and numerous other engineering components involving

two surfaces of contact under load and in relative motion [11]. In addition, titanium nitride coated or formed materials are being used for cutting and forming tools [12].

There are several successful studies of TiN production on titanium or Ti-6Al-4V substrates reported including, for instance, reactive sputtering [12, 13], physical vapor deposition (PVD) [14], chemical vapor deposition (CVD) [15], plasma assisted chemical vapor deposition (PACVD) [16], ion implantation and pulse ion implantation [17], laser nitriding [18, 19] and plasma ion nitriding [20, 21]. The first four methods are deposition processes and will produce a discrete TiN film on the substrate while ion implantation is a physically driven line-off-sight process. Pulse ion implantation can provide a three dimensional coverage, but the process still has a depth limitation and produces a fine distribution of TiN products rather than continuous compound layer [11]. Nitriding of titanium by laser treatment gives crack free hard surfaces, but the hardness increment is less than that obtained from ion nitriding. Conventional ion nitriding is an alternative process to produce titanium nitride at the surface of titanium and titanium alloys. Several, successful, previous attempts have been reported on the ion nitriding of titanium alloys [11, 20, 21]. Ion nitriding of titanium has been found to produce a thin surface layer of TiN (δ) followed by Ti_2N (ε) layer and an interstitial nitrogen diffusion zone in the adjacent α-Ti matrix. Plasma ion nitriding makes use of a glow discharge phenomenon to produce an energetic flux of nitrogen ions and neutrals that heats the work-piece, sputter cleans the surface, supplies active nitrogen and provides the energy for compound formation.

Although extensive use of Ti and Ti alloys exist both in the as received and nitrided cases, the expense is still such that the use of solid Ti or a Ti alloy is as high as 40 times that of a quality steel that it replaces in a given application [1]. The purpose of the present study was to weld Ti-6Al-4V alloy to 304 stainless steel plate and to pursue nitriding of the alloy, at different temperatures and times, by d.c. plasma ion nitriding. Although many successful studies have been reported for nitriding Ti and its alloys, there are no reported attempts is present to nitride and characterize Ti-6Al-4V alloy that was explosively joined to a 304 austenitic stainless steel plate. This is aimed at decreasing material cost and possibly increasing its implementation. The study also sought to characterize the surfaces and interfaces produced between Ti-6Al-4V and stainless steel in terms of microstructure and resulting properties.

2. Experimental
2.1. Explosive welding
A parallel explosive welding arrangement was used to explosively weld Ti-6Al-4V to 304 austenitic stainless steel (3.5 mm thick by 150×150 mm in dimensions). The steel was used as the flyer plate and the Ti-6Al-4V (1.5 mm thick) as the base plate. Steel and Ti-6Al-4V plates were placed in machined pockets in a containment plate 7.25 mm thick by 15×15 mm in dimensions. It was determined from previous experiments that explosive frame heights and stand-off-distances that produced detonation velocities of 2300–2500 ms^{-1} and flyer plate velocities of 425–510 ms^{-1} resulted in high strength Ti-6Al-4V/304 stainless steel welds with no defects. The explosive used for the experiment was
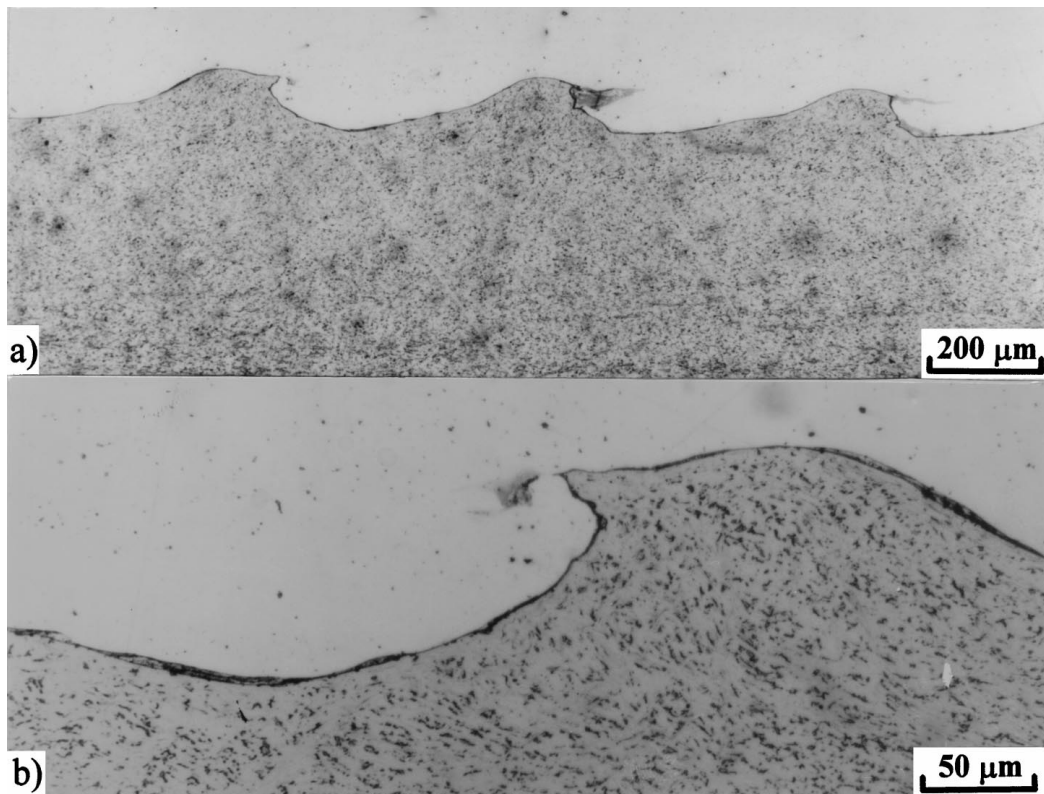

Figure 1 Ti-6Al-4V/304 stainless steel interface showing a slightly wavy interface morphology prior to ion nitriding.

ammonium nitrate-6% fuel oil (ANFO-6%). Following welding, explosively welded tandems were annealed for stress relief at 500 °C for 2 h duration in an argon atmosphere, in a tube furnace.

2.2. Ion nitriding conditions
Specimens used for ion nitriding were of $30 \times 30 \times 5$ mm in dimension. The specimens were ground, prior to nitriding, using 600 grit SiC paper and the Ti-6Al-4V layers were polished with 6 and 1 μm diamond cloth. All the specimens were ultrasonically cleaned in acetone at room temperature and rinsed in methanol. The plasma surface treatment was performed in a d.c plasma system which is described in [22]. The d.c. voltage was adjusted between 500 and 800 V, to obtain the prescribed nitriding temperature. The system was
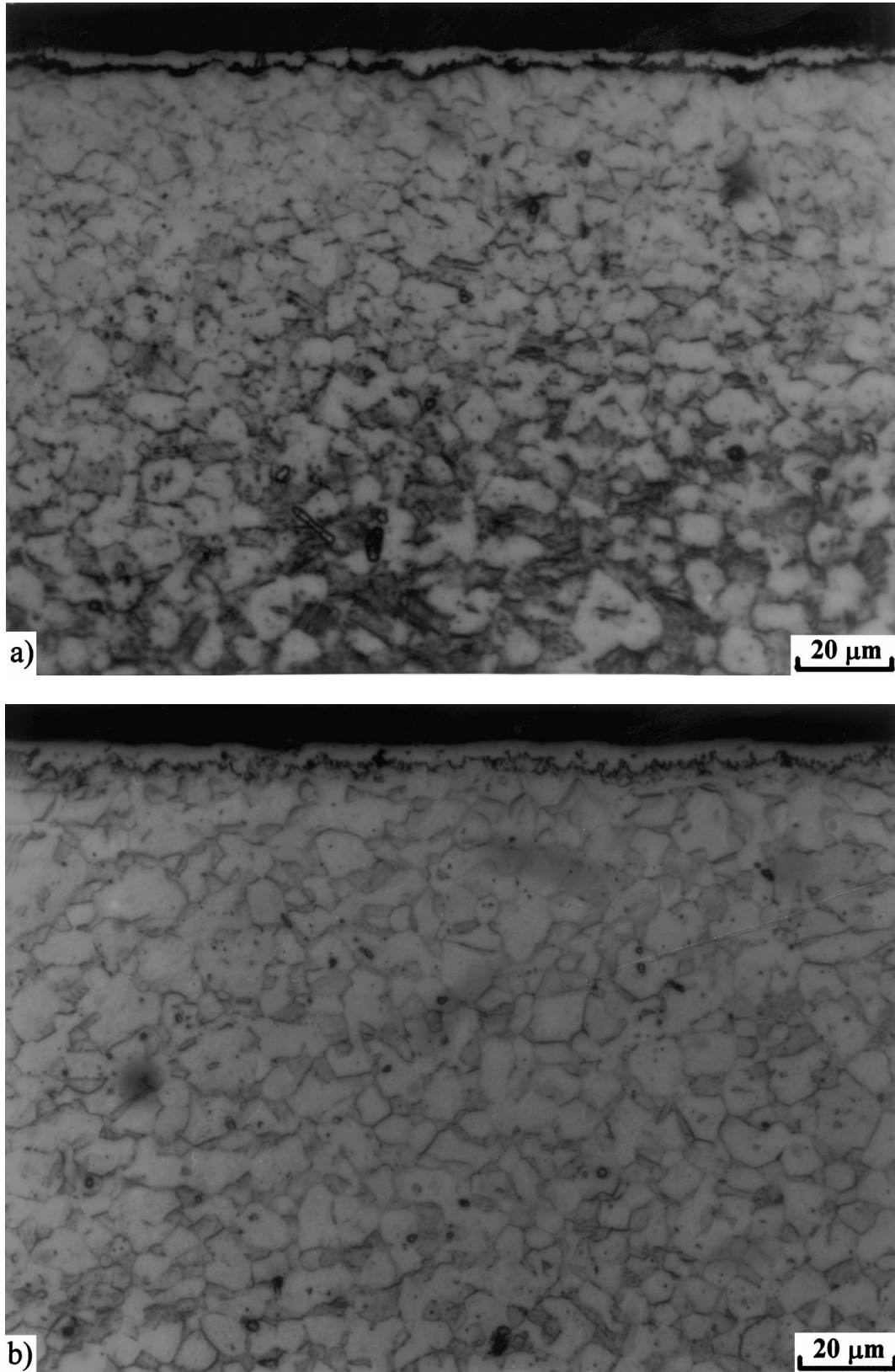

Figure 2 Optical micrographs of the cross-sections of Ti-6Al-4V alloy ion nitrided for 6 h at; (a) 700 °C, (b) 800 °C and (c) 900 °C.
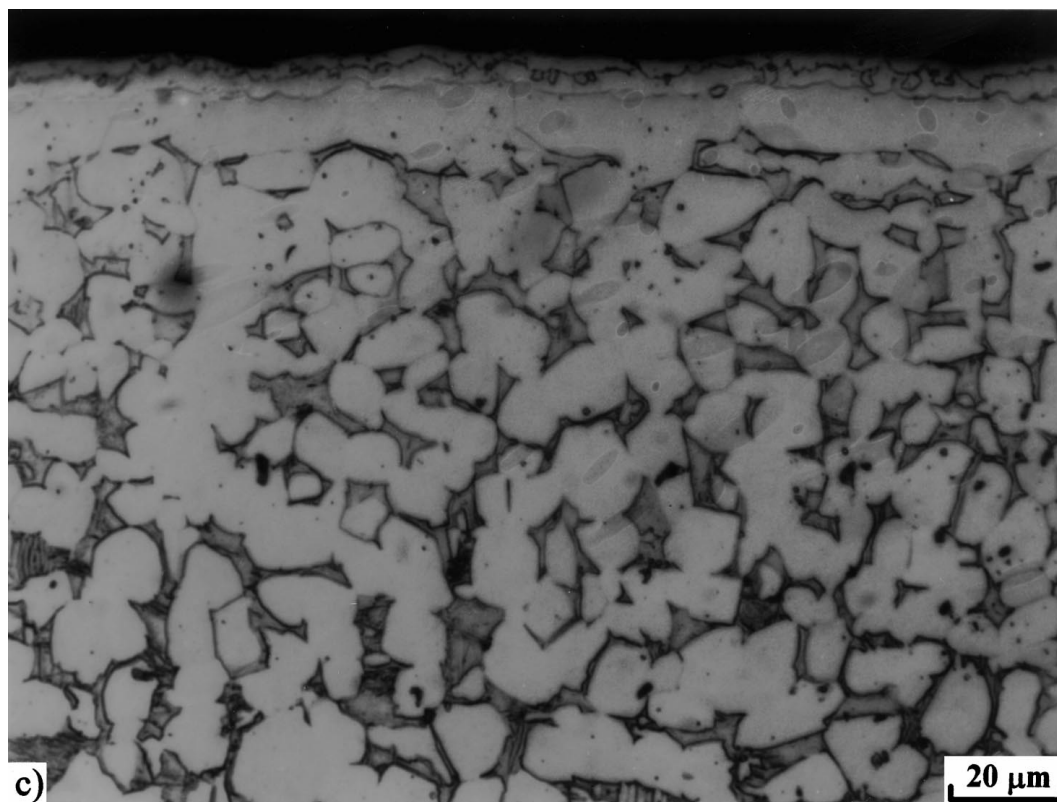
c)

20 μm

Figure 2 (*Continued*).

maintained at a (+) potential and work-pieces to be nitrided were placed on the cathode. The system was evacuated to 10^{-5} Torr pressure and backfilled with Ar for sputtering. Specimens were first sputtered in an Ar atmosphere (99.999%) pumped for two hours and then nitrogen gas was backfilled for ion nitriding. The nitriding was carried out at 5 Torr nitrogen partial pressure with 99.999% purity nitrogen gas. Argon and nitrogen gases were both flowed through a gas purifier operated at approximately 550 °C to eliminate residual oxygen. The nitriding temperature was measured using both a chromel alumel thermocouple, placed at the bottom of the nitrided sample and with an optical pyrometer. The nitriding temperatures were controlled by changing the power input. After 2 h of Ar sputtering at each nitriding condition, nitriding treatments were carried out at temperatures of 700, 800 and 900 °C as measured by a thermocouple and an optical pyrometer. The nitriding periods were chosen as 3, 6, 9 and 12 h for each temperature studied. After nitriding, an attractive gold colour was observed on the sample surfaces. Energy for substantial diffusion of nitrogen into the Ti-6Al-4V work pieces, welded to 304 stainless steel substrates, is assumed to be provided by the kinetic energy transfer generated by the ion bombardment [11].

2.3. Characterization

The cross-sectional samples of nitrided pieces were mounted in a bakalite/SiC mixture to ensure edge retention. Specimens were ground through successive SiC paper grades of 120, 240, 320, 400 and 600, and polished with 6 and 1 μm diamond clothes and finally finished with 0.05 μm alumina cloth. Polishing times were limited to 45–60 s on each wheel in order to avoid the onset of unacceptable bevelling of the specimen edges. Specimens were not rotated between grinding grades to prevent fracture of the thin nitrided layers. After subsequent cleaning with methanol in an ultrasonic cleaner, the nitrided samples were etched in a mixture of 1.0 ml HF, 2 ml HNO_3 and 50 ml H_2O. The thickness of various layers formed during ion nitriding was measured by an optical microscope and scanning electron microscopy (SEM). In addition, the thicknesses of the nitrided layers in the samples were measured with optical and SEM micrographs to obtain an accurate thickness. X-ray diffraction (XRD) analyse were performed for phase identification. The microhardnesses of the nitrided samples and weld interfaces, between Ti-6Al-4V alloy and 304 stainless steel, were determined by means of a LECO M-400 microhardness tester. A Knoop microhardness indenter was also used to provide indentation depths across various layers. A 50 g load was applied for 15 s for measuring the surface hardnesses of the nitrided samples. However, cross sectional and interface zone hardness measurements were made by applying a 100 g load for 15 s. Since the sample surfaces of the nitrided pieces were already polished prior to nitriding, the nitrided surfaces were perfectly polished for surface hardness measurements; only the use of 0.25 μm diamond cloth was needed to reveal a smooth and shiny surface.

3. Results
3.1. Microstructural features

Metallographic examination of the welded interface, between Ti-6Al-4V alloy and 304 stainless steel,

shows the interface to exhibit a slight waviness, although with no vorticity that can be delineated at even high magnifications. Figs 1a and b show the as welded microstructures at two different magnifications following the etching of the Ti-6Al-4V plate. The absence of vortex formation, melting or intermetallic formation is quite evident.

Plasma nitrided Ti-6Al-4V at 700, 800 and 900 °C for 3, 6, 9 and 12 h resulted in the formation of different phases depending on the treatment temperatures. The cross-sectional micrographs show that increasing the nitriding temperature caused the formation of several distinct phases in the nitrided case. Fig. 2 shows optical micrographs of the cross-sections of samples, which
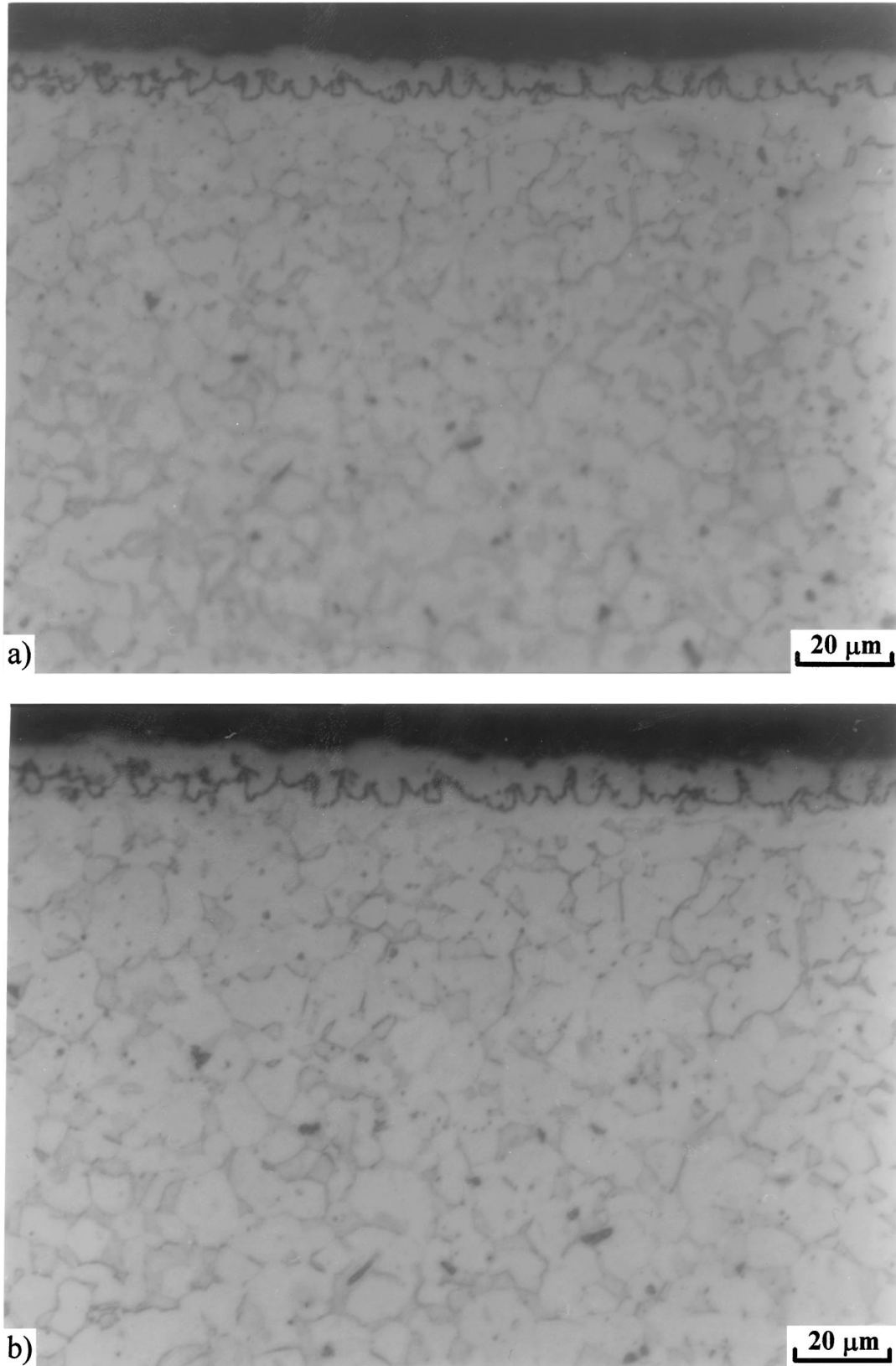

Figure 3 Optical micrographs of the cross-sections of Ti-6Al-4V alloy ion nitrided for 12 h at; (a) 700 °C, (b) 800 °C and (c) 900 °C.
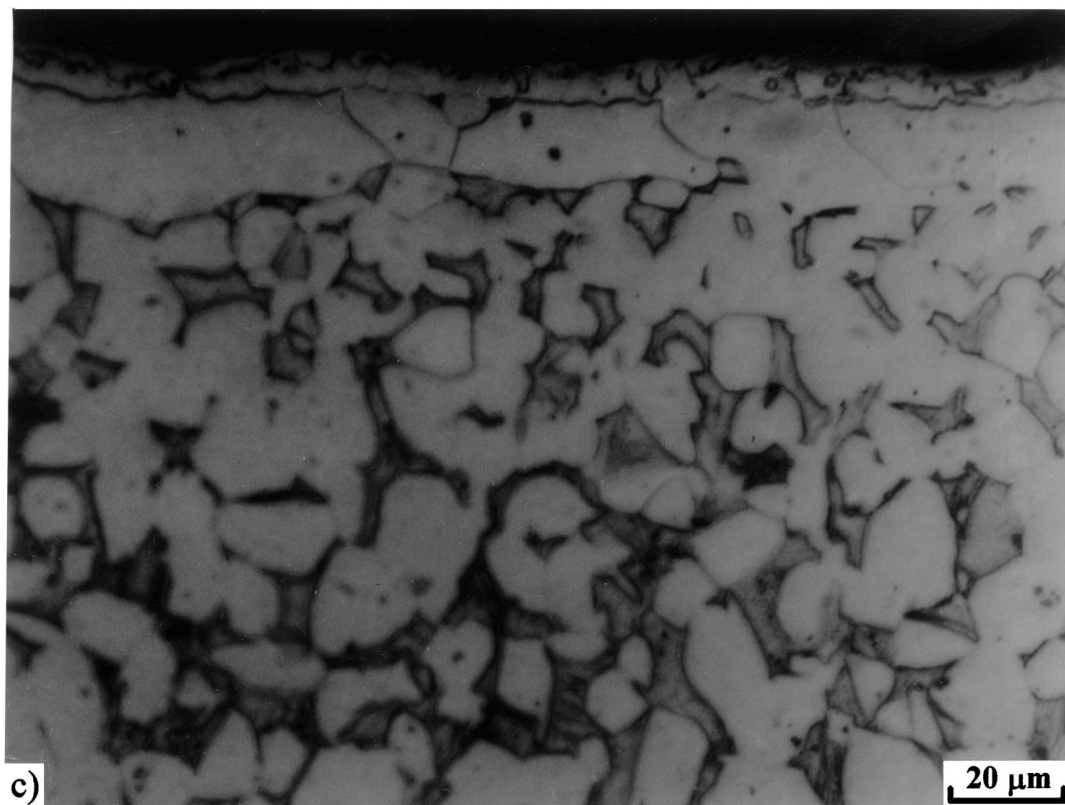
c)

20 μm

Figure 3 (Continued).

were nitrided at 700, 800 and 900 °C for 6 h. In addition, Fig. 3 presents ion nitrided cross-sections, for 12 h at 700, 800 and 900 °C. Figs 2 and 3 reveal that nitride layers grew parallel to the surface of the work pieces. The overlayers consist of TiN (δ) phase followed by a layer of Ti$_2$N (ε) and subsequently a thick layer of solid solution of nitrogen in Ti starting from outer surface. Although these distinct layers are not clearly seen in the optical micrographs of samples nitrided at 700, and 800 °C, they were verified by the XRD diffraction analysis. The formation of these layers is consistent with the phase diagram of Ti-N [23] and previous successful Ti nitriding studies [11, 20, 21]. Figs 2 and 3 show that increasing the nitriding temperature and time caused a gradual increase in the thickness of the nitrided layers. The increase in the nitriding temperature resulted in the clear appearance of δ, ε, and α-Ti solid solution phases. To reveal these distinct phases to be seen more visible in the specimen, a sample was nitrided at 900 °C, for 12 h; its microstructure is illustrated in Fig. 4 at two magnifications. Fig. 4a is the low magnification image of the microstructure which shows the top surface layer to consist of TiN and Ti$_2$N precipitation, followed by a nitrogen stabilized single phase α solid solution. Below this region, the recrystallized α phase can be clearly seen. The volume fraction of the β phase increases as the nitrogen content decreases. Finally, the core of the specimen contains the equilibrium $\alpha + \beta$ mixture. As shown in Fig. 4b, a thin δ phase is clearly seen in the optical micrograph as the light section on the edge. The intermediate ε phase is more prominent in the microstructure of Ti-6Al-4V alloy, nitrided at 900 °C. Fig. 5 shows SEM cross-sectional view of nitrided Ti-6Al-4V, at 900 °C for 6 h. In Fig. 5, at the edge of the cross-section, δ-TiN and ε-Ti$_2$N phases are formed as

a compound layers and followed by a solid solution of α-Ti.

To support the microstructural findings, XRD analysis were performed. For brevity, only the XRD pattern of 6 and 12 h nitrided samples, at 700 and 900 °C, are illustrated in Figs 6 and 7 respectively. All ion nitrided samples showed the presence of δ-TiN and ε-Ti$_2$N phases in their compound layers. Increasing the nitriding temperature and time resulted in the increase of the growth of δ-TiN and ε-Ti$_2$N phases and decrease in the α-Ti phase. Especially at low temperatures, a tetragonal (b.c.) VN phase developed in (002) peak. Increasing nitriding temperature caused a gradual decrease in the VN peaks. Samples nitrided at 900 °C, for 12 h, showed no indication of VN phase in the XRD analysis. XRD patterns reveal that, in all the nitrided work-pieces, the δ phase developed a strong (200) peak whereas the ε phase developed strong (111) and weaker (002), (311), (202) and (213) at 700 °C nitriding conditions. Increasing the nitriding temperature resulted in a strong δ (002) peak and weaker (111), (311) and (202) peaks.

3.2. Growth kinetics

Kinetics of nitride layer growth on Ti-6Al-4V, present material was studied for the layer composed of $\delta + \varepsilon$, named herein as the compound layer, and for the overall nitrogen rich layer starting from the edge of the $\alpha + \beta$ core structure and compound layer. This composite layer is called the case thickness or case depth. As shown in Figs 8a and b, the growth of the compound layer ($\delta + \varepsilon$) and the case depth ($\varepsilon + \delta +$ (nitrogen diffused α-rich structure)) obeyed a simple $t^{1/2}$ relationship. Nitriding of the Ti-6Al-4V alloy for 3 h produces
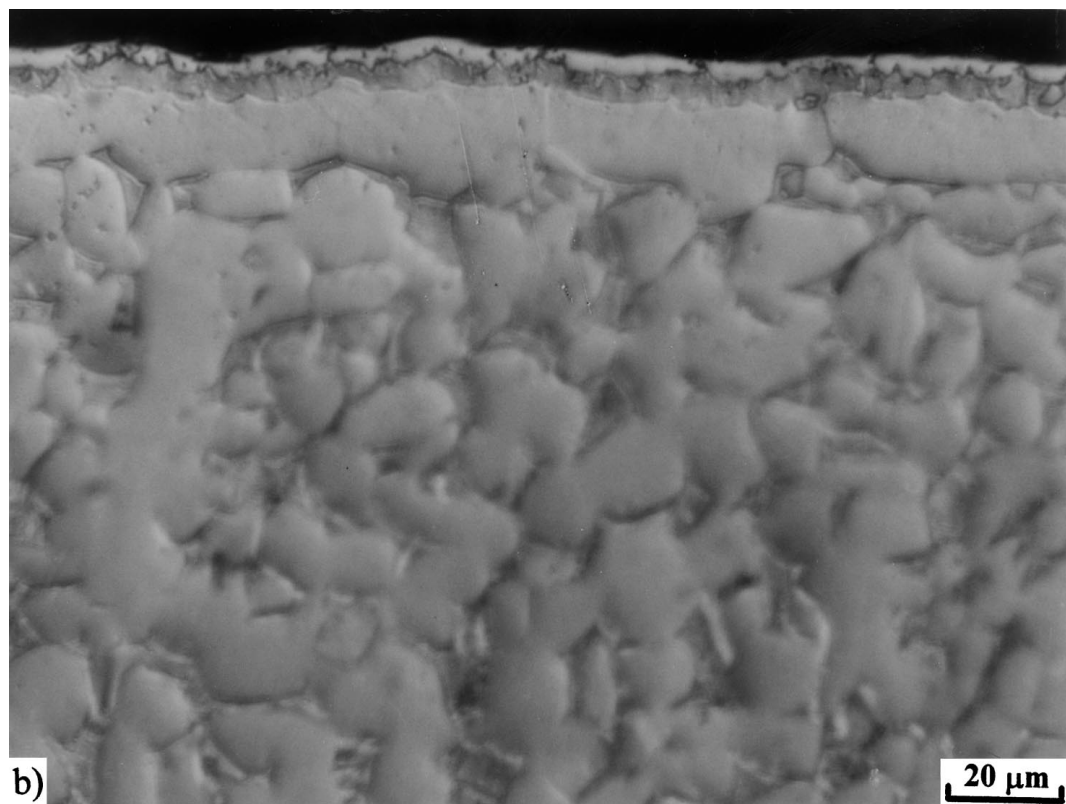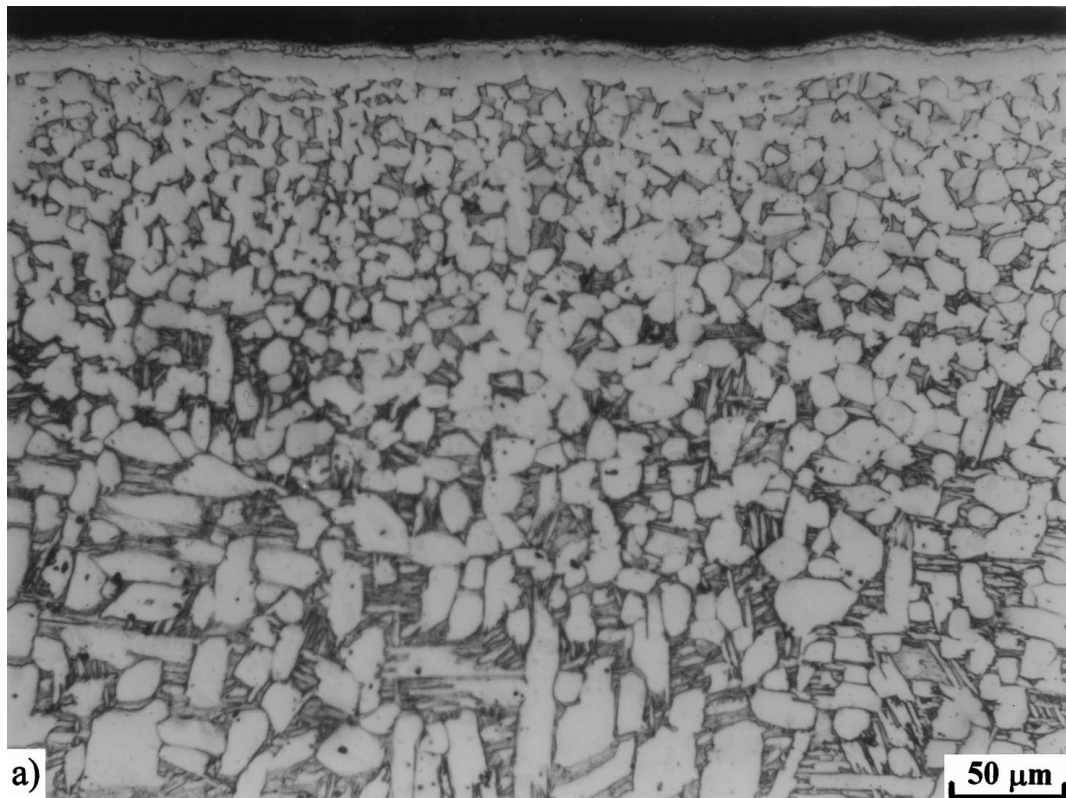
Figure 4 Optical micrographs of the cross-sections of Ti-6Al-4V alloy ion nitrided at 900 °C for 12 h showing; (a) the nitrided case and (b) compound layer.

a 1.73 μm compound layer at 700 °C. Increasing nitriding temperature to 900 °C gives 4.38 μm thickness in compound layer for the 3 h nitrided sample. Increasing nitriding temperature and time, thus, resulted in the gradual increase in compound layer which reached 9.62 μm for the sample nitrided at 900 °C for 12 h. Similarly, increasing temperature and time caused an increment in the case thickness which measured approximately 200 μm at 900 °C for 12 h nitrided sample.

3.3. Hardness measurements
To evaluate the effects of nitriding time and temperature on the extent of nitrogen diffusion, microhardness
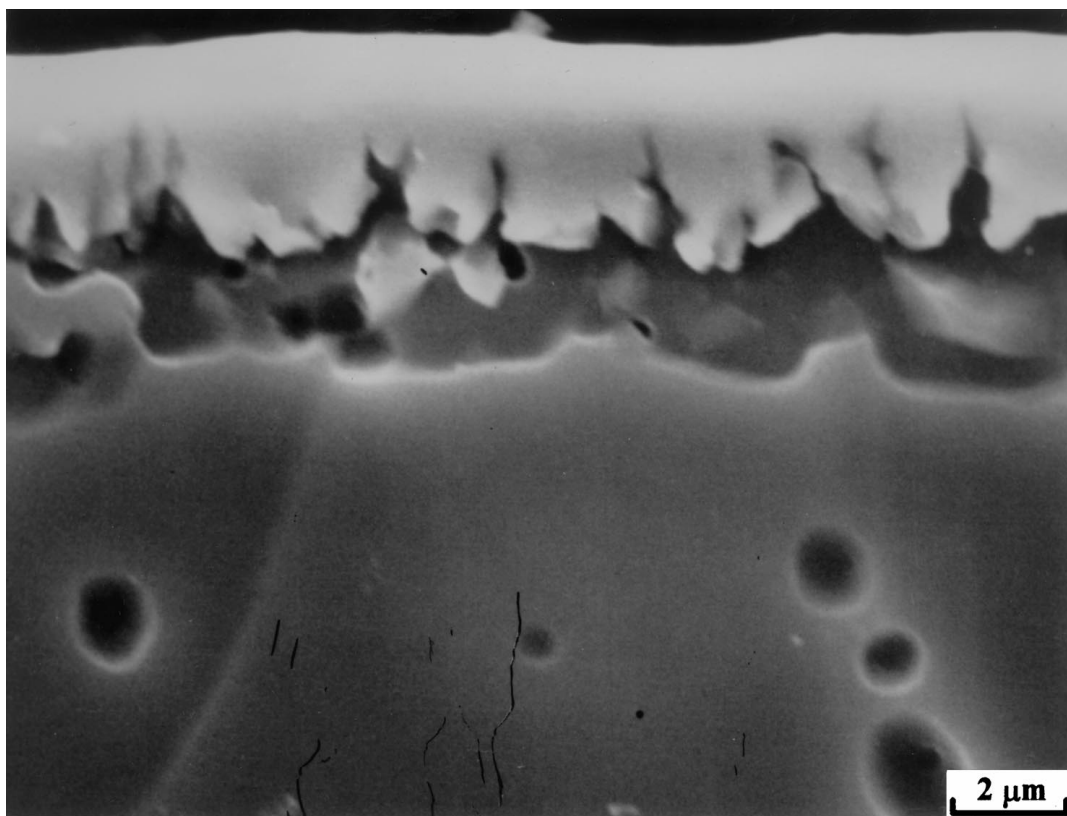
Figure 5 SEM micrograph of the cross-section of Ti-6Al-4V alloy ion nitrided at 900 °C for 6 h.

transverses were carried out on samples which were treated at 700, 800 and 900 °C for different exposure times. The effect of nitriding temperature on the microhardness of Ti-6Al-4V is illustrated in Fig. 9. For brevity, only the microhardness values of the samples that were nitrided for 3 and 12 h are presented. A significant increase in the Knoop hardness, up to 2520 kg/mm^2, is observed in the nitrided surfaces when compared with about 384 in the original sample that was explosively welded to 304 stainless steel. Nitriding at high temperatures also resulted in high hardness values. Even at lower temperatures (700 °C) as values high as 1714 hardness value were obtained. Nitriding at 900 °C for 12 h produced maximum surface hardness values around 2520, which is at least a sixfold increase over the original microhardness of the unprocessed specimen.

Interface hardness values between Ti-6Al-4V and 304 stainless steel were measured and only the results of the sample that nitrided at 900 °C for 12 h are presented in Fig. 10. The microhardness profiles, in Fig. 10, for the as welded and nitrided transition joints, the hardness values decreased with an increase in treatment temperature, possibly due to an annealing effect. Microscopic observations showed no extraneous phase formation that could be detected at the interface after ion nitriding. Samples that were treated at 800 and 900 °C, for long exposure times, showed a slight amount of recrystallization adjacent to the interface in the Ti alloy. However, hardness values at the interfaces were still higher than core hardnesses for either the Ti-6Al-4V alloy and the stainless steel.

4. Discussion

Microscopic examinations, XRD analysis and microhardness evaluations on cross-sections of nitrided specimens indicated the formation of two nitride layers (δ-TiN and ε-Ti$_2$N) followed by an interstitial nitrogen diffusion zone in the Ti-6Al-4V alloys ion nitrided subsequent to their explosive welding onto 304 stainless steel plates. Similar observations have been made previously following ion nitriding of the same alloy at high temperatures (800 to 900 °C) [22, 24]. Fig. 11 shows this layer morphology in a fractured cross-section of a nitrided Ti-6Al-4V specimen. The compound layer (δ-TiN and ε-Ti$_2$N) has separated from the α-Ti solid solution during this severe fracturing of the sample. Aforementioned studies, based on nitriding of Ti and Ti alloys, showed a gradual increment of the hardness in the nitrided layers [11, 20]. In general, Ti-6Al-4V alloys produced higher hardness values than pure Ti alloys. Metin and Inal [20] obtained 1700 HV for Ti and Ti-6242S alloy with 1080 °C nitriding temperature. Kembaiyan *et al*. [21] measured a maximum of 1800 Knoop microhardness value for Ti-6Al-4V alloy nitrided at 900 °C for 16 h. Muraleedharan and Meletis [11] obtained around 1500 HV values for Ti-6Al-4V alloy nitrided by intensified plasma at 480 °C for 16 h. The present results showed 700–1000 higher microhardness values when compared with these studies. This is believed, herein, to be due to the shock wave induced generation of excessive defect substructure, which is stable during processing, and this leads to its continual contribution to enhanced nitrogen diffusion.

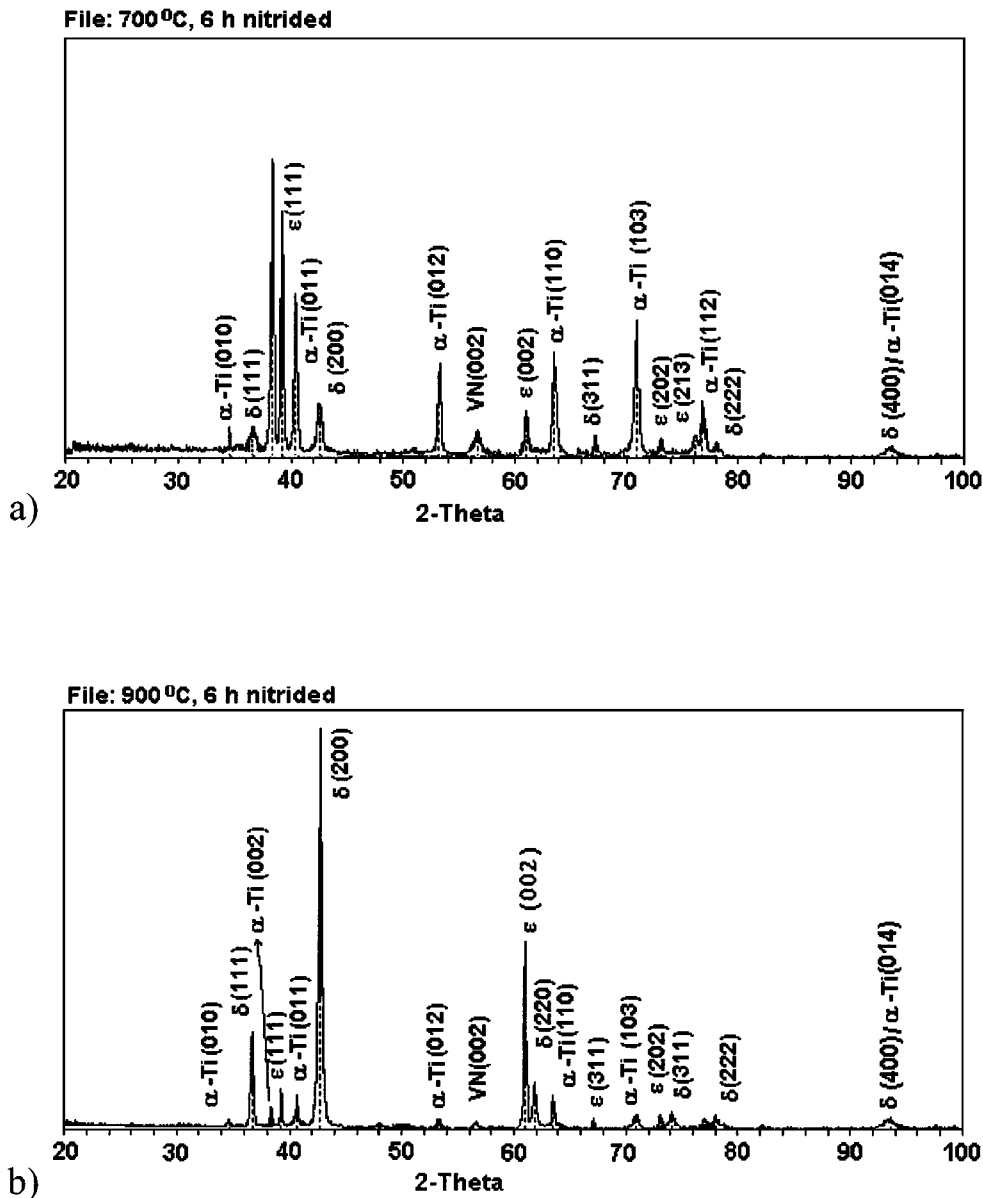Ti-6Al-4V alloys have been reported to show tremendous response to ion nitriding. It was reported by

Figure 6 XRD patterns for Ti6-Al-4V alloy ion nitrided for 6 h at; (a) 700 °C and (b) 900 °C.

Muraleedharan and Meletis [11] that the compound layer in pure titanium is always thicker than that of Ti-6Al-4V, whereas the opposite was pointed out for the diffusion layer. Similar observations have been made by Rie and Lampe [24]. Boriskina *et al*. [25] found that aluminum additions to titanium increase the nitrogen diffusion rate. Rie and Lampe [24] reported that, in the titanium alloys, that contain some of aluminum, Ti_2AlN phase is formed beneath the TiN and Ti_2N layers. In the dual $(\alpha + \beta)$ phase alloys the aluminum stabilizes the α phase, while vanadium acts as a β stabilizer. Precipitation of AlN in the nitrogen rich case or formation of Ti_2AlN are possible but these phases were not seen in our XRD analysis. As indicated in the XRD patterns, especially for samples produced at low temperatures, the VN phase with a tetragonal b.c. crystal structure was identified in the surfaces of the nitrided sample. Increasing the nitriding temperature resulted in decrease and even disappearance of this nitride phase at 900 °C treatment temperatures. Kembaiyan *et al*. [21] carried out microanalysis along the cross-section using wavelength dispersive spectrometry (WDS), on the

Ti-6Al-4V alloy nitrided for 16 h at 900 °C. WDS analysis revealed the depletion of vanadium in the nitrided layer of Ti-6Al-4V. They further substantiated the partitioning of vanadium by Auger electron spectroscopy (AES), which showed a significant vanadium peak to be present in the core of the sample but its disappearance in the nitrided layers. The depletion of vanadium in the vicinity of the surface thus stabilizes the HCP α phase and nitriding results in mainly the formation of a solid solution of nitrogen in the α phase. This possibly is one of the reasons that case thicknesses increase to approximately 200 μm in this Ti-6Al-4V alloy. XRD results showed strong peaks of (200) for δ-TiN and (111) for ε-Ti_2N. The high intensity peaks of the nitrides is expected to have a significant effect on the properties of the nitrided materials. For example, Matthews [26] has shown that a (111) texture of the TiN has an adverse effect on its wear resistance. The present results indicate that explosive welding and subsequent nitriding produces more desirable nitride orientations and a beneficial effect on the properties is expected.
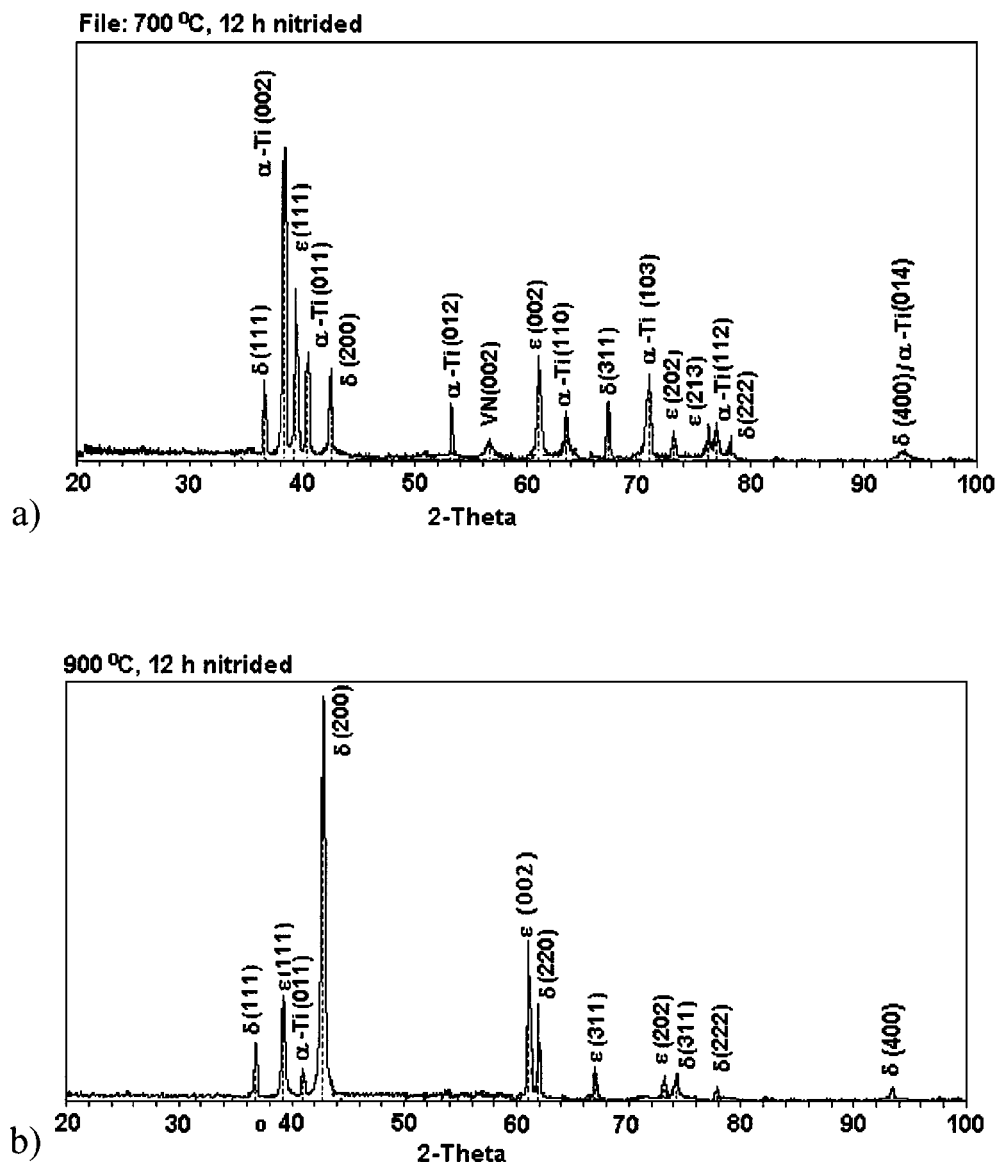
Figure 7 XRD patterns for Ti6-Al-4V alloy ion nitrided for 12 h at; (a) 700 °C and (b) 900 °C.

In explosively treated metals, dislocation and point defect substructures are generated by the passage of shock waves [27]. Kressel and Brown [28] reported that vacancy and interstitial concentrations are three to four times higher after shock loading than after cold rolling. The enhancement in nitrogen diffusion observed herein is believed to be due to the shock loading generated defect substructure, as stated earlier. In the present study, the thicker compound and case layers and related higher hardness values are consistent with this hypothesis. Because of this high defect concentration, it is believed that the formation of VN also took place and the synergism of the dual nitride formation resulted in the much higher hardness values. This was also observed in our previous studies that incorporated Al, Cr and Al + Cr as the nitridable specie content of steels ion nitrided [29]. XRD results did not show any AlN and Ti_2AlN phases in the present work and, transmission electron microscopy (TEM) studies are needed to investigate the presence of these nitrides.

Shock loading in explosive welding results in extensive work hardening of the welded metal components. This is easily verifiable through increased hardness of the component metals. In the present work, the hardness of Ti-6Al-4V alloy was measured as 384 by Knoop indention after explosive welding treatment. The as-received hardness of Ti-6Al-4V alloys hase been reported to be between 300 and 350 HV [11, 21]. The high hardnesses obtained in the present study may be another advantage that results in the maintenance of high hardness values after the nitriding procedure. It is reported by Yasumaru *et al.* [30] that cracking occurs in TiN films owing to the plastic deformation of substrates and thus, the good contribution of TiN formation cannot be realized. The fact that an extensive defect substructure, induced by shock wave passage, was in existence in our samples possibly led to better accommodation of the TiN precipitates since no cracking was observed in our microstructures.

5. Conclusions

1. Ti-6Al-4V alloy, explosively welded onto a 304 stainless steel plate was successfully ion nitrided in a d.c. plasma system. An attractive gold colour on the samples was produced by this process.
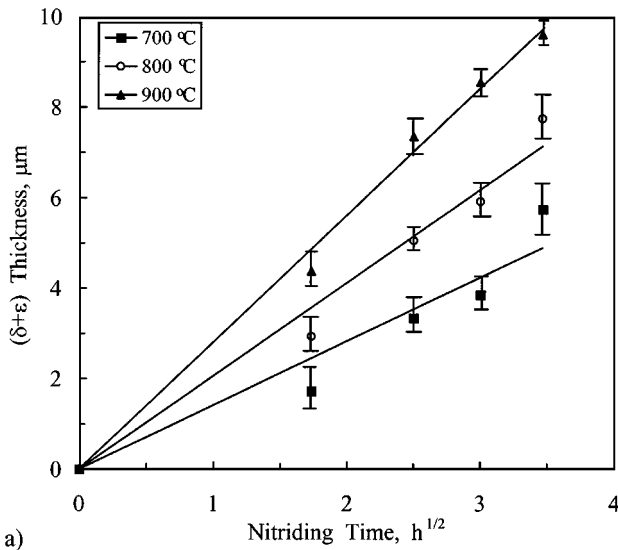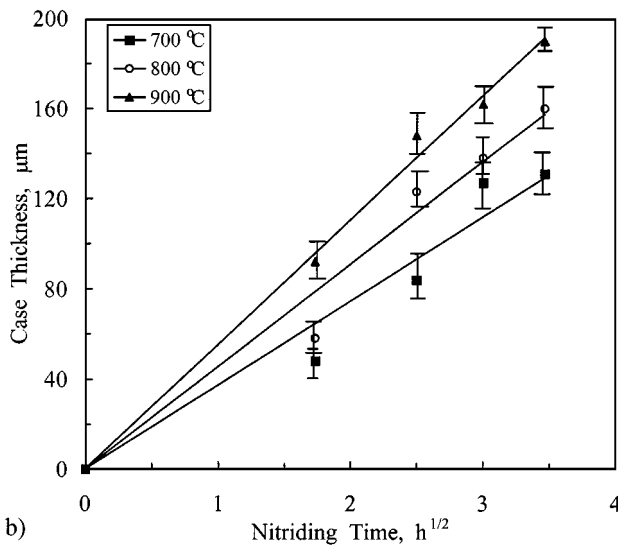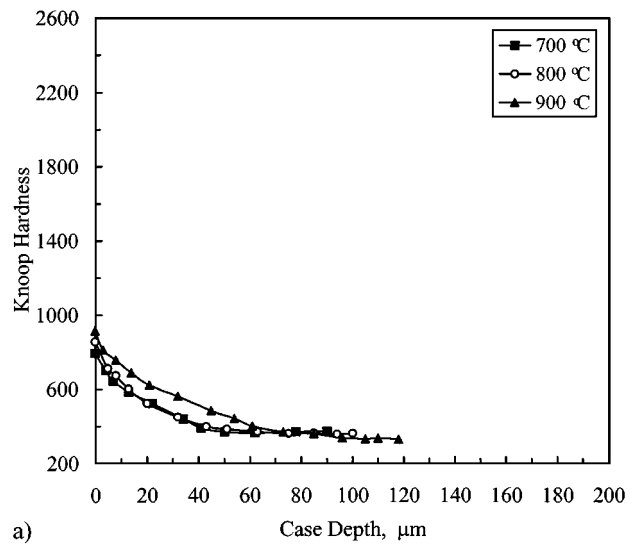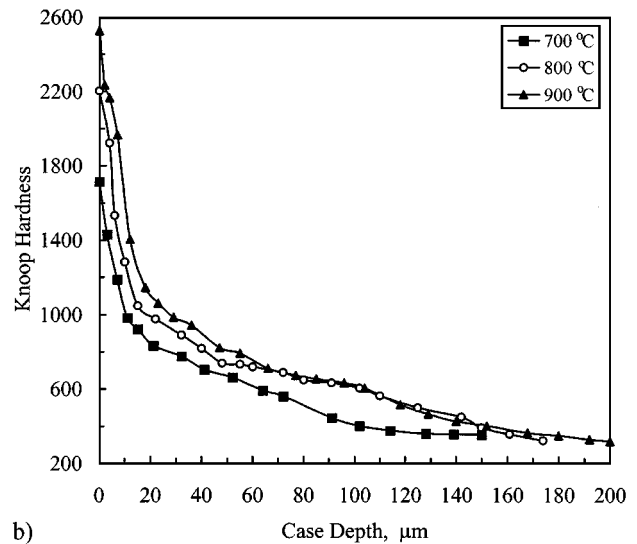
Figure 8 Growth of (a) compound layer ($\delta + \varepsilon$) and (b) nitrided case as a function of processing time and temperature in Ti-6Al-4V alloy welded to 304 stainless steel.

Figure 9 Variation of microhardness across the cross-section of the ion nitrided Ti-6Al-4V samples at 700, 800 and 900 °C temperatures for; (a) 3 h and (b) 12 h ion nitriding times.

2. The compound layer ($\delta + \varepsilon$) and the case depth were determined to be approximately 10 and 200 μm respectively. These large thickness values were attributed to the higher diffusion rate afforded of the high dislocation density and vacancy concentration produced by shock waves during explosive welding.

3. In explosively welded Ti-6Al-4V samples, ion nitriding offers a hard case, as high as 2520 Knoop hardness, as compared to 384 of the unprocessed sample.

4. Various layers, TiN, Ti_2N and a solid solution of nitrogen in the α phase, in sequence from the surface, were identified by XRD. XRD analysis also showed the presence of the VN phase, especially at low nitriding temperatures.

5. Optical metallography and microhardness measurements showed that growth rate of nitrided layers is controlled essentially by volume diffusion of nitrogen through the nitrided layer.

6. Ion nitriding of explosively welded Ti-6Al-4V onto a 304 stainless steel plate, could lead to a reduced cost expense of this materials in use and to material coverage with Ti-alloys that afford benefit of a high
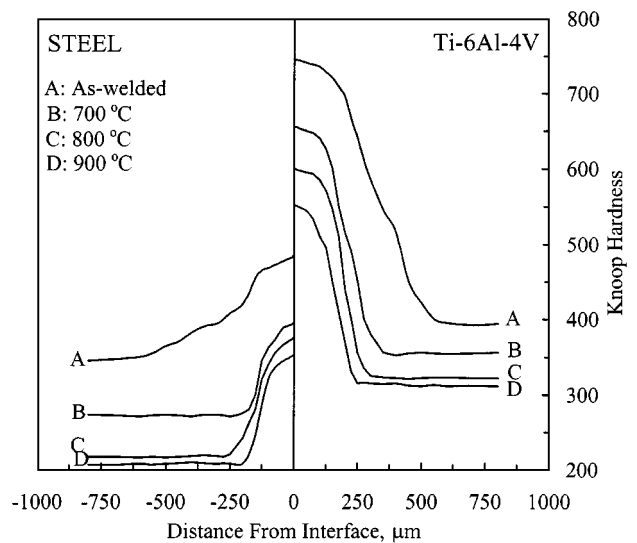

Figure 10 As-welded and ion nitrided Ti-6Al-4V/304 stainless steel interface; Knoop microhardness profiles showing the effect of nitriding temperature and time to the interface and bulk materials in the 12 h nitrided condition.
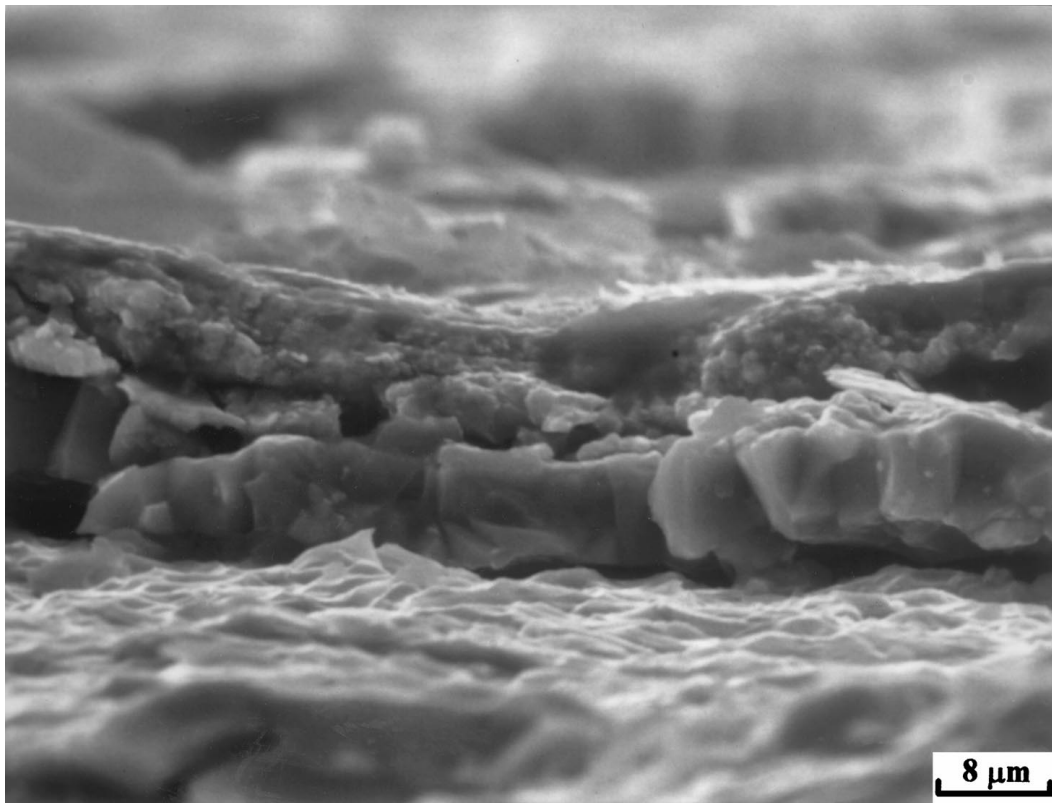
Figure 11 SEM micrograph showing the compound layer ($\delta + \varepsilon$) and α-Ti phase separated from each other in the fractured surface of a sample nitrided for 12 h at 900 °C.

hardness with good toughness of a core for structural applications.

Acknowledgment

References

1. O. T. INAL, A. SZECKET, D. J. VIGUERAS and H. PAK, *J. Vac. Sci. Technol.* **A3** (1985) 2605.
2. T. IZUMA, K. HOKAMOTO, M. FUJITA and M. AOYAGI, *Trans. Japan Welding Society* **23** (1992) 33.
3. C. A. ZIMMERLY, O. T. INAL and R. H. RICHMAN, *Mater. Sci. Eng.* **A188** (1994) 251.
4. H. MICHEL, T. CZERWIEC, M. GANTIOS, D. ABLITZER and A. RICHARD, *Surface and Coating Technol.* **72** (1995) 103.
5. L. BAUFRAY, F. A. HOULE and R. J. WILSON, *J. Appl. Phys.* **61** (1987) 4640.
6. M. WAUTELET, *J. Appl. Phys. A* **50** (1990) 131.
7. A. ANTTILA, J. RAISANEN and J. KEINONEN, *Appl. Phys. Lett.* **42**(6) (1983) 489.
8. A. S. KORHONEN, E. H. SIRVIO and M. S. SOLONEN, *Thin Solid Films* **107** (1983) 387.
9. B. K. PAWLAK and W. ZYRICKI, *ibid.* **230** (1990) 115.
10. R. G. VARDIMAN and R. A. KONT, *J. Appl. Phys.* **53** (1982) 690.
11. T. M. MURALEEDHARAN and E. I. MELETIS, *Thin Solid Films* **221** (1992) 104.
12. L. PETROV, L. HULIMAN, U. HELMERSSON, J. E. SUDGREN and J. E. GREENE, *ibid.* **169** (1989) 299.
13. W. D. SPROUL, P. J. RUDNIK and C. A. GOGOL, *ibid.* **171** (1989) 171.
14. J. E. SUNDGREN, *ibid.* **128** (1985) 21.
15. A. AGUERO and P. LOWDEN, in "Surface Modification Technologies, IV," edited by T. S. Jundarshan, D. G. Bhat and M. Jeandin (TMS and Materials Society, 1991) p. 817.
16. J. LAIMER, H. STORI and P. RODHAMMER, *Thin Solid Films* **191** (1990) 77.
17. M. NUNOGAKI, H. SUEZAWA, Y. KURATOMI and K. MIYAZAKI, *Vacuum* **39**(2–4) (1989) 281.
18. S. MRIDHA and T. N. BAKER, *Mater. Sci. Eng.* **A188** (1994) 224.
19. P. LAURENS, H. L. ENFANT, M. C. S. CATHERINE, J. J. BLECHET and J. AMOUROUX, *Thin Solid Films* **293** (1997) 220.
20. E. S. METIN and O. T. INAL, *Mater. Sci. Eng.* **A145** (1991) 67.
21. K. T. KEMBAIYAN, R. D. DOHERTY, R. P. SINGH and R. VERMA, in "Proceedings of the 2nd Ion Nitriding and Ion Carburizing," edited by T. Spalvanis and W. L. Kovacs (TMS, 1990) p. 119.
22. E. S. METIN and O. T. INAL, *Metall. Trans.* **A20** (1989) 1819.
23. ASM Handbook, Vol. 3, Alloy Phase Diagram, ASM, The Materials Information Society, 1992, pp. 2–999.
24. K. T. RIE and T. LAMPE, *Mater. Sci. Eng.* **69** (1985) 473.
25. N. G. BORISKINA, D. P. SHASKOW, E. M. KENINA and V. M. MIKHALIN, *Mater. Sci. Heat. Treat.* **23** (1981) 503.
26. A. MATTHEWS, *J. Vac. Sci. Technol.* **A3** (1985) 2534.
27. T. Z. BLAZYNSKI, "Explosive Welding. Forming and Compaction" (Applied Science Publishers, New York, 1983) p. 62.
28. H. KRESSEL and N. J. BROWN, *J. Appl. Phys.* **38** (1967) 1618.
29. O. T. INAL and E. S. METIN, in "Proceedings of the Plasma and Laser Processing of Materials," edited by K. Upadhya (TMS, 1991) p. 225.
30. N. YASUMARU, K. TSUCHIDA, E. SAJI and T. IBE, *Mater. Trans. JIM* **34** (1993) 696.